

Constrained Output Feedback Control of a Multivariable Polymerization Reactor

Michael J. Kurtz, Guang.-Yan Zhu, and Michael A. Henson, *Member, IEEE*

Abstract—A multivariable nonlinear control strategy which accounts for unmeasured state variables and input constraints is developed for the free-radical polymerization of methyl methacrylate in a continuous stirred tank reactor. Monomer concentration and reactor temperature are controlled using a technique which combines nonlinear input–output decoupling and linear model predictive control. Input constraints are handled explicitly by applying linear model predictive control to the constrained linear system obtained after feedback linearization and constraint transformation. Unmeasured initiator and solvent concentrations are accounted for by treating the live polymer concentration as an unknown parameter which is estimated on-line. The performance of the control strategy is compared to other nonlinear control techniques through closed-loop simulations.

Index Terms—Chemical industry, multivariable systems, nonlinear systems, output feedback, process control.

I. INTRODUCTION

POLYMERIZATION reactors are difficult to control effectively due to their highly nonlinear behavior. Two important problems which sometimes are neglected in academic studies of polymerization reactor control are lack of on-line measurements and input constraints. Consider a typical free-radical polymerization system. Reactor temperature is readily measured, and monomer concentration usually can be inferred from other measurements. However, accurate and reliable measurements of initiator concentration and solvent concentration are difficult to obtain with available on-line sensors [2]. Furthermore, potential manipulated inputs such as monomer feed concentration and coolant temperature are subject to constraints dictated by operational limitations.

Most nonlinear control techniques proposed for polymerization reactors are based on feedback linearization [7], [8] or nonlinear model predictive control (NMPC) [13]. A serious disadvantage of NMPC is the need to solve a nonlinear programming problem on-line at each sampling period. This makes NMPC computationally expensive and potentially unreliable as the nonlinear program may converge to a local minimum or even diverge. On the other hand, feedback linearization is an analytical design method which yields easily implementable nonlinear control laws if the system is input–output decouplable and possesses stable zero dynamics.

Several applications of feedback linearizing control to continuous polymerization reactors have been presented. Daoutidis *et al.* [5] consider the problem of designing a multivariable, feed-forward–feedback controller for a free-radical polymerization reactor. The problems of unmeasured state variables and input constraints are not addressed. These same issues are neglected in the polymerization reactor control study presented by Alvarez *et al.* [3]. McAuley and MacGregor [12] propose a nonlinear control method which utilizes an extended Kalman filter (EKF) to estimate disturbances and remove offset due to plant/model mismatch. The EKF is not used to provide estimates of unmeasured state variables. To account for input saturation a simple optimization problem which penalizes instantaneous deviations of the outputs from their setpoint values is proposed. This method is similar to nonlinear antiwindup techniques [10] it provides only *indirect* compensation for saturation constraints and does not provide any means of handling rate-of-change input constraints or output constraints.

Adebekun and Schork [1], [2] investigate some polymerization reactor control problems associated with input multiplicities and propose the use of a least-squares control technique to regulate four outputs with three inputs. Unmeasured state variables are estimated using a EKF, but the control technique does not provide explicit compensation for input constraints. Soroush and Kravaris [19] conducted an experimental test of a nonlinear multivariable control technique for a free-radical polymerization reactor in which the problems of unmeasured variables and input constraints are addressed. Unmeasured state variables are estimated via a reduced order open-loop nonlinear observer. This approach has several drawbacks, including the possibility of biased estimates and the lack of a tuning parameter which allows the convergence rate of the estimation error to be adjusted. Input constraints are handled by eliminating integral action in the nonlinear controller whenever a constraint is active. Although this method of indirect constraint compensation is adequate for the tests shown, it is expected that a technique which *explicitly* accounts for input constraints can provide improved performance over a wider range of operating conditions.

Previously, we have developed an explicit constraint compensation technique for single input–single output (SISO) systems under full-state feedback via feedback linearization and linear model predictive control (FBL-MPC) [11]. Using a chemical reactor example, it was demonstrated that the combined FBL-MPC technique provided superior performance to linear model predictive control methods based on Jacobian linearization [15] and successive linearization about the current operating point [6]. In this paper, we develop a multivariable extension of the FBL-MPC control strategy for the free-radical

Manuscript received October 7, 1997; revised January 1, 1999. Recommended by Associate Editor, T. Ogunnaike.

The authors are with the Department of Chemical Engineering, Louisiana State University, Baton Rouge, LA 70803-7303 USA (e-mail: henson@che.lsu.edu).

Publisher Item Identifier S 1063-6536(00)01018-6.

polymerization of methyl methacrylate in a continuous reactor. The technique accounts for unmeasured state variables as well as input constraints. A feedback linearizing controller compensates for process nonlinearities, and a linear model predictive controller compensates for input constraints transformed into the feedback linearized space. Unmeasured solvent and initiator concentrations are handled by treating the live polymer concentration as an unknown parameter which is estimated on-line from available measurements. Simulation studies are used to compare the proposed control strategy to alternative constraint handling techniques for nonlinear systems.

II. POLYMERIZATION REACTOR MODEL

The process considered is the free-radical polymerization of methyl methacrylate in a constant volume continuous stirred tank reactor. The model equations are [2]

$$\begin{aligned}\dot{M} &= \frac{q}{V}(M_f - M) - k_p MP \\ \dot{T} &= \frac{q}{V}(T_f - T) + \left(\frac{-\Delta H}{\rho c_p}\right) k_p MP - \frac{hA_c}{V\rho c_p}(T - T_c) \\ \dot{I} &= \frac{q}{V}(I_f - I) - k_d I \\ \dot{S} &= \frac{q}{V}(S_f - S)\end{aligned}\quad (1)$$

where M is the monomer concentration, T is the reactor temperature, I is the initiator concentration, S is the solvent concentration, V is the reactor volume, q is the feed flow rate, M_f is the monomer feed concentration, T_f is the feed temperature, I_f is the initiator feed concentration, S_f is the solvent feed concentration, and T_c is the coolant temperature. Other model parameters are defined in [2]. The live polymer concentration P is calculated via the following equation:

$$P = \sqrt{\frac{2fk_d I}{k_t}} \quad (2)$$

where f is the initiator efficiency.

The associated rate expressions are

$$\begin{aligned}k_d &= k'_d \exp\left(-\frac{E_d}{RT}\right) \\ k_p &= k'_p \exp\left(-\frac{E_p}{RT}\right) \\ k_{t_o} &= k'_{t_o} \exp\left(-\frac{E_{t_o}}{RT}\right).\end{aligned}\quad (3)$$

The expression for k_t is obtained using (3) and the Schmidt-Ray correlation for the gel effect [18]

$$g_t = \frac{k_t}{k_{t_o}} = \begin{cases} 0.10575 \exp[17.15V_f - 0.01715(T - 273.2)] \\ V_f > [0.1856 - 2.965 \times 10^{-4}(T - 273.2)] \\ 2.3 \times 10^{-6} \exp[75V_f] \\ V_f \leq [0.1856 - 2.965 \times 10^{-4}(T - 273.2)]. \end{cases} \quad (4)$$

The glass effect correlation g_p sometimes used for the propagation rate constant ($k_p = g_p k_{p_o}$) is set to unity as this is a good assumption except when the reactor fluid is extremely viscous

(i.e., low solvent fraction) [1], [9]. The free volume V_f is calculated from the volume fractions of monomer, polymer, and solvent in the reactor through the following equations [2], [18]:

$$\begin{aligned}\Omega &= V_{f_m} \phi_m + V_{f_p} \phi_p + V_{f_s} \phi_s \\ V_f &= \begin{cases} \Omega, & \text{if } \Omega > 0 \\ 0, & \text{if } \Omega \leq 0 \end{cases}\end{aligned}\quad (5)$$

where

$$\begin{aligned}V_{f_m} &= 0.025 + 0.001(T - 167) \\ V_{f_p} &= 0.025 + 0.00048(T - 387) \\ V_{f_s} &= 0.025 + 0.001(T - 181).\end{aligned}\quad (6)$$

Volume fractions are calculated using the reactor concentrations and physical property data under the assumption of ideal mixing

$$\begin{aligned}\phi_m &= \frac{MW_m M}{\rho_m} \\ \phi_i &= \frac{MW_i I}{\rho_i} \\ \phi_s &= \frac{MW_s S}{\rho_s} \\ \phi_p &= \frac{\rho - \phi_m \rho_m - \phi_s \rho_s - \phi_i \rho_i}{\rho_p}\end{aligned}\quad (7)$$

where MW_j is the molecular weight of species j , ρ_j is the pure component density of species j , and ρ is the density of the fluid in the reactor (which is assumed to be constant). The equation for ϕ_p is derived from the requirement that the mass fractions in the reactor sum to unity. The initiator concentration in the reactor usually is very low relative to the other species. As a result, it is reasonable to make the approximation $\phi_i = 0$.

Perfect control of the reactor volume via manipulation of the solvent flow rate is assumed. As a result, the feed concentrations of the individual species are not independent. In particular, the mass fractions of the feed stream must sum to unity. This means the feed solvent concentration S_f is a function of the feed monomer and feed initiator concentrations

$$S_f = \frac{\rho}{MW_s}(1 - V_{if} - V_{mf}) \quad (8)$$

where V_{if} and V_{mf} are the volume fractions of initiator and monomer in the feed stream, respectively.

The polymerization reactor equations (1) are nondimensionalized to give the following state-space model [2]:

$$\begin{aligned}\frac{dx_1}{d\tau} &= x_{1f} - x_1 - Da_p W(x) x_1 E_x(x_2) \\ \frac{dx_2}{d\tau} &= x_{2f} - x_2 + B Da_p \gamma_p W(x) x_1 E_x(x_2) + \beta(x_{2c} - x_2) \\ \frac{dx_3}{d\tau} &= x_{3f} - x_3 - Da_d x_3 E_{x_d}(x_2) \\ \frac{dx_4}{d\tau} &= x_{4f} - x_4\end{aligned}\quad (9)$$

where

$$\begin{aligned}E_x(x_2) &= \exp\left[\frac{x_2}{1 + \frac{x_2}{\gamma_p}}\right] \\ E_{x_d}(x_2) &= \exp\left[\frac{\gamma_d x_2}{1 + \frac{x_2}{\gamma_p}}\right].\end{aligned}\quad (10)$$

TABLE I
DIMENSIONLESS VARIABLES

| Dimensionless Variable | Definition |
|------------------------|---|
| τ | $\frac{tq}{V}$ |
| x_1 | $\frac{M}{M_{f0}}$ |
| x_2 | $\frac{T-T_f}{T_f} \frac{E_p}{RT_f}$ |
| x_3 | $\frac{I}{M_{f0}}$ |
| x_4 | $\frac{S}{M_{f0}}$ |
| W | $\frac{P}{M_{f0}}$ |
| x_{1f} | $\frac{M_f}{M_{f0}}$ |
| x_{2c} | $\frac{T_c-T_f}{T_f} \frac{E_p}{RT_f}$ |
| x_{2f} | $\frac{T_f-T_f}{T_f} \frac{E_p}{RT_f}$ |
| x_{3f} | $\frac{I_f}{M_{f0}}$ |
| x_{4f} | $\frac{S_f}{M_{f0}}$ |
| B | $\frac{(-\Delta H)M_{f0}}{\rho c_p T_f}$ |
| β | $\frac{hA_c}{\rho c_p q}$ |
| γ_p | $\frac{E_p}{RT_f}$ |
| γ_d | $\frac{E_d}{E_p}$ |
| η | $\frac{k'_d e^{-\gamma_d \gamma_p}}{k'_p M_{f0} e^{-\gamma_p}}$ |
| Da_p | $k'_p e^{-\gamma_p} M_{f0} \frac{V}{q}$ |
| Da_d | ηDa_p |

A description of the dimensionless variables is given in Table I. While not given here for the sake of brevity, the auxiliary equations for free volume, reaction rates, and solvent feed concentration also are nondimensionalized.

The molecular weight distribution (MWD) is largely determined by the first three moments of the distribution which often are called the principle moments. Differential equations describing the evolution of the principal moments are derived in [1] and [18] for methyl methacrylate polymerization. In this application, the principle moments are *unique* functions of the reactor state variables x_1 – x_4 at steady state [1]. It is easy to verify that the steady-state values of the initiator concentration (x_3) and the solvent concentration (x_4) are given by the following equations:

$$\begin{aligned} \bar{x}_3 &= \frac{x_{3f}}{1 + Da_d E_{x_d}(\bar{x}_2)} \\ \bar{x}_4 &= x_{4f} = c_1 + c_2 x_{1f} + c_3 x_{3f} \end{aligned} \quad (11)$$

where

$$\begin{aligned} c_1 &= \frac{\rho}{M_{f0} MW_s}, \quad c_2 = -\left(\frac{\rho}{\rho_m}\right) \left(\frac{MW_m}{MW_s}\right) \\ c_3 &= -\left(\frac{\rho}{\rho_i}\right) \left(\frac{MW_i}{MW_s}\right). \end{aligned} \quad (12)$$

These functions depend uniquely on the model parameters, the feed conditions, and the temperature \bar{x}_2 . Thus, the MWD can be approximately controlled by driving the monomer concentration (x_1) and the reactor temperature (x_2) to particular setpoints as long as the feed conditions are constant. This implies that polymer grades corresponding to different steady-state reactor conditions but the same feed conditions can be produced using monomer concentration and reactor

temperature as the controlled variables and monomer feed concentration and coolant temperature as the manipulated variables. For the more general case (i.e., polymers corresponding to different feed conditions), this is not necessarily true due to the coupling of monomer concentration and monomer feed concentration which introduces the possibility of multiple steady-state values of the solvent concentration.

III. NONLINEAR CONTROL SYSTEM DESIGN

In this section, a multivariable, nonlinear controller is designed for the polymerization reactor presented in the previous section. The controller design procedure used is analogous to the method of feedback linearization with linear model predictive control for SISO systems previously presented by the authors [11]. The major contributions of this paper are that the method is extended to multivariable processes and used to solve an important polymerization reactor control problem.

For some polymerization reactors, the controlled outputs are chosen to include moments of the MWD [16]. We do not follow this approach because it is difficult to obtain accurate and reliable on-line measurements of MWD moments. Initiator concentration is another common controlled output because it has a strong effect on the molecular weight distribution through the live polymer concentration P . However, initiator concentration is more difficult to measure on-line, thereby necessitating the use of state estimation. In general, controlling the initiator estimate will lead to offset in the actual variable. As shown above, the initiator concentration is a unique function of the reactor temperature at equilibrium. All these factors contribute to the choice of monomer feed concentration and coolant temperature as manipulated inputs and monomer concentration and reactor temperature as controlled outputs.

Therefore, the objective is to control monomer concentration ($y_1 = x_1$) and reactor temperature ($y_2 = x_2$) by manipulating monomer feed concentration ($u_1 = x_{1f}$) and coolant temperature ($u_2 = x_{2c}$). We assume the availability of on-line measurements of monomer concentration (x_1) and reactor temperature (x_2); the initiator concentration (x_3) and solvent concentration (x_4) are assumed to be unmeasurable. For convenience, the nondimensional reactor equations (9) are written as

$$\begin{aligned} \dot{x}_1 &= f_{11}(x_1) + f_{12}(x_1, x_2)W(x) + u_1 \\ \dot{x}_2 &= f_{21}(x_2) + f_{22}(x_1, x_2)W(x) + \beta u_2 \\ \dot{x}_3 &= f_{31}(x_2, x_3) \\ \dot{x}_4 &= f_{41}(x_4) + \delta u_1 \end{aligned} \quad (13)$$

where $W(x)$ is the dimensionless live polymer concentration, which is a function of the unmeasurable state variables x_3 and x_4 ; δ is a known constant that appears due to the solvent feed relation (8); and the functions $f_{ij}(\cdot)$ follow from (8) and (9).

A. Feedback Linearization

Nonlinear controller design is based on input–output decoupling [8]. Consider a control-affine nonlinear system with m inputs and m outputs

$$\begin{aligned} \dot{x} &= f(x) + \sum_{i=1}^m g_i(x)u_i \\ y_i &= h_i(x) \quad i = 1, 2, \dots, m. \end{aligned} \quad (14)$$

The input–output decoupling control law is [7]

$$u = \begin{bmatrix} L_{g_1} L_f^{r_1-1} h_1(x) & \cdots & L_{g_m} L_f^{r_m-1} h_m(x) \\ \vdots & \ddots & \vdots \\ L_{g_1} L_f^{r_1-1} h_1(x) & \cdots & L_{g_m} L_f^{r_m-1} h_m(x) \end{bmatrix}^{-1} \left(\begin{bmatrix} v_1 \\ \vdots \\ v_m \end{bmatrix} - \begin{bmatrix} L_f^{r_1} h_1(x) \\ \vdots \\ L_f^{r_m} h_m(x) \end{bmatrix} \right) \equiv D^{-1}(x)[v - b(x)] \quad (15)$$

where $[r_1 \cdots r_m]^T$ is the vector relative degree, $L_f^{r_j} h_j(x)$ and $L_{g_i} L_f^{r_j-1} h_j(x)$ are Lie derivatives of the scalar function $h_j(x)$, and v is a $m \times 1$ vector of new manipulated inputs. If the decoupling matrix $D(x)$ is nonsingular, the control law is well defined and a suitable change of coordinates $[\xi \ \eta]^T = \Phi(x)$ yields a closed-loop system in the normal form [7]

$$\begin{aligned} \dot{\xi} &= A\xi + Bv \\ y &= C\xi \\ \dot{\eta} &= q(\xi, \eta, v). \end{aligned} \quad (16)$$

If we define $r = r_1 + \cdots + r_m$, then: ξ and η are r -dimensional and $(n - r)$ -dimensional state vectors, respectively; the triplet (A, B, C) is in Brunovsky block canonical form; and $q(\cdot)$ is a vector of nonlinear functions which characterize the zero dynamics [8]. It can be shown that the zero dynamics of the polymerization reactor model are locally stable at the steady states considered in Section IV.

For the polymerization reactor model given by (13), the input–output decoupling control law is

$$u = B^{-1}[v - a_1(x_1, x_2) - a_2(x_1, x_2)\hat{W}] \quad (17)$$

where

$$a_1(x_1, x_2) = \begin{bmatrix} f_{11}(x_1) \\ f_{21}(x_2) \end{bmatrix}, \quad a_2(x_1, x_2) = \begin{bmatrix} f_{12}(x_1, x_2) \\ f_{22}(x_1, x_2) \end{bmatrix} \\ B = \begin{bmatrix} 1 & 0 \\ 0 & \beta \end{bmatrix}. \quad (18)$$

The variable \hat{W} represents an estimate of the live polymer concentration $W(x)$, which is unknown because the initiator and solvent concentrations are unmeasurable. Although \hat{W} can be generated by explicitly estimating x_3 and x_4 , this approach requires the design of a nonlinear state estimator such as an extended Kalman filter [14]. As discussed below, we utilize a simpler adaptive approach in which W is viewed as an unknown parameter.

The vector of new inputs (v) typically is used to place the closed-loop poles and to provide integral action in the nonlinear control law [8]. In the absence of constraints this simple approach usually is sufficient to provide good performance. However, in the presence of active constraints this method can result in very poor (and even unstable) closed-loop responses due to the input being “clipped” [11]. We propose using linear model predictive control [15] to provide explicit compensation

for input constraints. As shown below, the main challenge of this technique is to transform the constraints on u to constraints on v .

B. Parameter Estimation

The live polymer concentration $W(x)$ is an unknown quantity since it is a function of the unmeasured state variables x_3 and x_4 . Rather than design a nonlinear observer to generate the unmeasured variables, we estimate W directly using on-line parameter estimation. This approach is justified theoretically if W changes “slowly” with respect to time [17]. Although this does not strictly hold for the polymerization reactor studied here, the simulation results in Section IV show the parameter estimator is able to track W sufficiently well to yield good closed-loop performance.

We utilize an indirect estimation technique since this allows considerable flexibility with respect to the controller design method. If direct adaptive control is used, the exact form of the control law must be specified *a priori*; this is not straightforward in the present application due to the use of linear model predictive control. Note that if the feed initiator concentration is chosen as a manipulated input, this estimation technique cannot be used and more complex nonlinear state estimation would be required. The following gradient update law is derived by assuming W is an unknown constant [17]

$$\begin{aligned} \dot{\hat{z}} &= -\alpha e + a_1(z) + a_2(z)\hat{W} + Bu \\ \dot{\hat{W}} &= -\gamma e^T a_2(z) \end{aligned} \quad (19)$$

where $z = [x_1 \ x_2]^T$, $\hat{z} = [\hat{x}_1 \ \hat{x}_2]^T$, $e = \hat{z} - z$, and $\alpha > 0$ and $\gamma > 0$ are tuning parameters.

C. Transformed System Equations

When linear model predictive control is applied to the feedback linearized system, it is necessary to map the constraints from the original input space to the feedback linearized space. This mapping is based on the transformed system equations obtained by applying the input–output decoupling control law to the nonlinear system. Therefore, these equations must be derived before linear model predictive control can be applied. From the standpoint of controller design the original system equations are

$$\begin{aligned} \dot{z} &= a_1(z) + a_2(z)W + Bu \\ \dot{\hat{z}} &= -\alpha e + a_1(z) + a_2(z)\hat{W} + Bu \\ \dot{\hat{W}} &= -\gamma e^T a_2(z). \end{aligned} \quad (20)$$

This form is obtained because W is assumed to be an unknown constant parameter rather than a state-dependent function. Using the fact that $y = z$, we can derive the associated normal form equations by choosing $\xi = z$ and $\eta = [\hat{z}^T \ \hat{W}]^T$. Application of the input–output decoupling control law (17) then yields

$$\begin{aligned} \dot{\xi} &= a_2(\xi)(W - \eta_3) + v \\ \dot{\eta} &= q(\xi, \eta, v) \end{aligned} \quad (21)$$

where

$$q(\xi, \eta, v) = \begin{bmatrix} -\alpha \begin{bmatrix} \eta_1 - \xi_1 \\ \eta_2 - \xi_2 \end{bmatrix} + v \\ -\gamma \begin{bmatrix} \eta_1 - \xi_1 & \eta_2 - \xi_2 \end{bmatrix} a_2(\xi) \end{bmatrix}. \quad (22)$$

Although this represents the true equations for the transformed space, the form obtained is not useful for constraint calculation because the equations contain the unknown variable W . To eliminate this variable, it is assumed that $W = \hat{W}$ (i.e., $W = \eta_3$) since the true value of the live polymer concentration is unknown. Therefore, the transformed system equations used for constraint calculation are

$$\begin{aligned} \dot{\xi} &= v \\ \dot{\eta} &= q(\xi, \eta, v). \end{aligned} \quad (23)$$

D. Linear Model Predictive Control

The monomer feed concentration (u_1) and the coolant temperature (u_2) are subject to hard constraints of the form

$$u_{1l} \leq u_1 \leq u_{1h}, \quad u_{2l} \leq u_2 \leq u_{2h}. \quad (24)$$

The goal is to apply linear model predictive control (LMPC) to the feedback linearized system to account for these constraints. Since LMPC is more naturally formulated in discrete time, the linear subsystem in (16) is discretized exactly with a sample-period T to yield

$$\begin{aligned} \xi(k+1) &= A_d \xi(k) + B_d v(k) \\ y(k) &= C \xi(k) \end{aligned} \quad (25)$$

where the matrices A_d and B_d follow directly from the continuous-time matrices A and B [4]. This model is used in the infinite horizon LMPC strategy proposed by Muske and Rawlings [15]. The open-loop optimal control problem can be expressed as

$$\begin{aligned} \min_{v(k|k)} \sum_{j=0}^{\infty} & [\xi(k+j|k) - \xi_s]^T Q [\xi(k+j|k) - \xi_s] \\ & + [v(k+j|k) - v_s]^T R [v(k+j|k) - v_s] \\ & + [v(k+j|k) - v(k+j-1|k)]^T S [v(k+j|k) \\ & - v(k+j-1|k)] \end{aligned} \quad (26)$$

where ξ_s and v_s are target values for ξ and v , respectively, and $Q \geq 0$, $R > 0$, $S \geq 0$ are tuning matrices. The decision vector is defined as $V(k|k) = [v^T(k|k), \dots, v^T(k+N-1|k)]^T$, where N is the control horizon. All future moves beyond the control horizon are set equal to the target value v_s . As discussed in [11], the matrix A_d is unstable and in order for the LMPC problem to have a feasible solution it is necessary to impose the equality constraint $\xi(k+N|k) = \xi_s$.

To obtain constraints on the new input v , the constraints on u are mapped into the feedback linearized space using a multi-variable extension of the procedure in [11]. As discussed below, this yields constraints of the following form:

$$v_l(k+j|k) \leq v(k+j|k) \leq v_h(k+j|k), \quad 0 \leq j \leq N-1. \quad (27)$$

The resulting optimization problem can be solved efficiently as a standard quadratic program [11].

Discretization of the decoupling control law (17) yields

$$v(k) = a_1[\xi(k)] + a_2[\xi(k)]\eta_3(k) + Bu(k). \quad (28)$$

The transformed constraints are determined at each sampling period by solving the following optimization problem subject to the inequality constraints (28):

$$\begin{aligned} v_l(k+j|k) &= \min_u a_1[\xi(k+j|k)] \\ &\quad + a_2[\xi(k+j|k)]\eta_3(k+j|k) + Bu \\ v_h(k+j|k) &= \max_u a_1[\xi(k+j|k)] \\ &\quad + a_2[\xi(k+j|k)]\eta_3(k+j|k) + Bu. \end{aligned} \quad (29)$$

Note that the variables $\xi(k+j|k)$ and $\eta_3(k+j|k)$ cannot be calculated until the input sequence is calculated, which is not possible until the constraints are specified. We address this difficulty by approximating the current input sequence with a shifted version of the sequence calculated at the last time step

$$\begin{aligned} V(k|k-1) &= [v(k|k-1) v(k+1|k-1) \cdots v(k+N-2|k-1) v_s]. \end{aligned} \quad (30)$$

As discussed in [11], the shifted input sequence can be used to integrate the normal form (23) with the initial condition $\xi(k|k-1) = \xi(k)$ and $\eta(k|k-1) = \eta(k)$ in order to obtain future values of the transformed state variables

$$\begin{aligned} Z(k|k-1) &= \\ & [\xi(k|k-1) \quad \xi(k+1|k-1) \quad \cdots \quad \xi(k+N-1|k-1)] \\ N(k|k-1) &= \\ & [\eta(k|k-1) \quad \eta(k+1|k-1) \quad \cdots \quad \eta(k+N-1|k-1)]. \end{aligned} \quad (31)$$

These predictions can be used in the optimization problem (29) in place of the actual values. Although this method yields approximate future constraints for v , the constraints calculated for the first input move correspond exactly to the actual constraints on u since the current measurements and estimates are used.

To remove offset caused by modeling errors, a disturbance model which assumes unmeasured disturbances enter through the state equations is introduced as described in [15]. The disturbances are estimated with a linear observer designed for the augmented system consisting of the linear state equations (25) and assumed state equations for the disturbances. The disturbances are assumed to be constant: $d(k+1) = d(k)$. The estimated disturbances \hat{d} are used to shift the target values ξ_s and v_s in the open-loop optimal control problem (26) as described in [11]. The disturbance estimator is tuned by choosing the desired eigenvalues λ of the associated closed-loop error equation.

IV. SIMULATION RESULTS

The combined feedback linearization/linear model predictive control (FBL-MPC) strategy is applied to the free-radical polymerization of methyl methacrylate as described by the dimen-

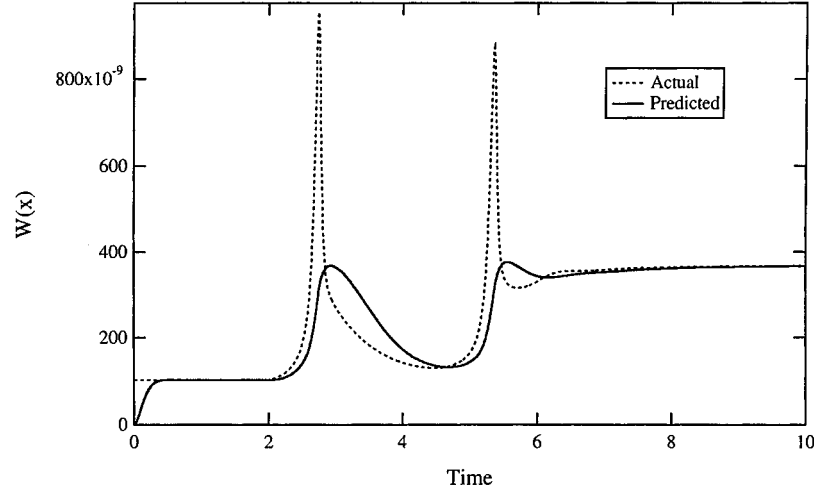


Fig. 1. Open-loop estimation of live polymer concentration.

TABLE II
NOMINAL OPERATING CONDITIONS AND PARAMETER VALUES

| Variable | Value | Variable | Value |
|-----------|--|----------|--|
| k'_d | $1.69 \times 10^{14} \text{ s}^{-1}$ | E_d | $30000 \frac{\text{cal}}{\text{mol}}$ |
| k'_p | $4.925 \times 10^5 \frac{\text{L}}{\text{mol} \cdot \text{s}}$ | E_p | $4353 \frac{\text{cal}}{\text{mol}}$ |
| k'_{to} | $9.80 \times 10^7 \frac{\text{L}}{\text{mol} \cdot \text{s}}$ | E_{to} | $701 \frac{\text{cal}}{\text{mol}}$ |
| Da_p | 5.871×10^6 | B | 0.3635 |
| Da_d | 3.6447×10^{11} | β | 1.3 |
| f | 0.5 | c_p | $0.4 \frac{\text{cal}}{\text{g} \cdot \text{K}}$ |
| MW_s | $88.10 \frac{\text{g}}{\text{mol}}$ | MW_m | $100.11 \frac{\text{g}}{\text{mol}}$ |
| MW_i | $242.23 \frac{\text{g}}{\text{mol}}$ | ρ_s | $901 \frac{\text{g}}{\text{L}}$ |
| ρ_m | $939 \frac{\text{g}}{\text{L}}$ | ρ_p | $1200 \frac{\text{g}}{\text{L}}$ |
| ρ | $1038 \frac{\text{g}}{\text{L}}$ | q | $0.2813 \frac{\text{L}}{\text{s}}$ |
| V | 900 L | T_f | 320 K |
| M_{f_0} | $4.5 \frac{\text{mol}}{\text{L}}$ | x_{1f} | 1.286 |
| x_{2f} | 0 | x_{3f} | 0.01429 |
| x_{4f} | 0.964 | x_{2c} | 0 |
| x_1 | 0.593 | x_2 | 0.75 |
| x_3 | 0.012 | x_4 | 1.865 |

sionless equations (9). The nominal operating point and parameter values are given in Table II. These values are taken from [2], with the exception that β which has been changed from 3.25 to 1.3 to reflect a smaller heat transfer rate. The manipulated inputs are constrained as follows:

$$0 \frac{\text{mol}}{\text{L}} \leq M_f \leq 9 \frac{\text{mol}}{\text{L}}, \quad 300 \text{ K} \leq T_c \leq 440 \text{ K} \quad (32)$$

which correspond to the following constraints on the dimensionless inputs:

$$0 \leq u_1 \leq 2.0535, \quad -0.42 \leq u_2 \leq 2.571. \quad (33)$$

The tuning parameters for the FBL-MPC controller (26) and the parameter update law (19) are chosen as

$$Q = I, \quad R = 5I, \quad S = I, \quad N = 20$$

$$\lambda = [0.4 \ 0.4]^T, \quad \alpha = 20, \quad \gamma = 4000. \quad (34)$$

The parameter estimator is initialized with $\hat{W}(0) = 0$, while the actual value is $W(0) = 10.132 \times 10^{-8}$. The sampling time (T) is chosen as 0.02 dimensionless time units in the subsequent simulations. A larger sampling time would reduce on-line computation at the expense of closed-loop performance.

The estimation of W under open-loop conditions is shown in Fig. 1. The inputs are initially set to the nominal values in Table II, and then are changed to [1.286 0.1] at $\tau = 2$ and [1.5 0.1] at $\tau = 5$. The estimate \hat{W} does not track the actual value during periods of rapid change caused by the input changes. However, the estimate converges rapidly to the actual value once the initial spike decays. This will be shown to be adequate for the FBL-MPC strategy. While improved estimates can be obtained using a higher adaptation gain γ , modeling errors typically preclude the use of high gains. It is important to note that all controllers discussed in this section use the same parameter update law and identical tuning parameters when possible.

The FBL-MPC strategy is compared to standard feedback linearization using pole placement and no constraint compensation (FBL-PP). Tests for the FBL-PP controller are shown in Figs. 2 and 3. The FBL-PP controller is tuned such that the dimensionless closed-loop time constant for each decoupled SISO loop is 0.2, which is approximately one-fifth the dominant open-loop time constant. This value of the closed-loop time constant gives very similar responses for the FBL-PP and FBL-MPC controllers in the absence of constraints.

Fig. 2 illustrates the inability of the FBL-PP controller to stabilize the nominal operating point in the presence of constraints. The incorrect initial parameter value $\hat{W}(0)$ causes the coolant temperature (u_2) to encounter the lower constraint. The controller is unable to recover as the gel effect becomes prevalent, and the monomer concentration (u_1) then saturates at its upper constraint. As a result, the outputs are unable to attain the setpoints. Also shown in Fig. 2 is the response of the FBL-PP controller in the

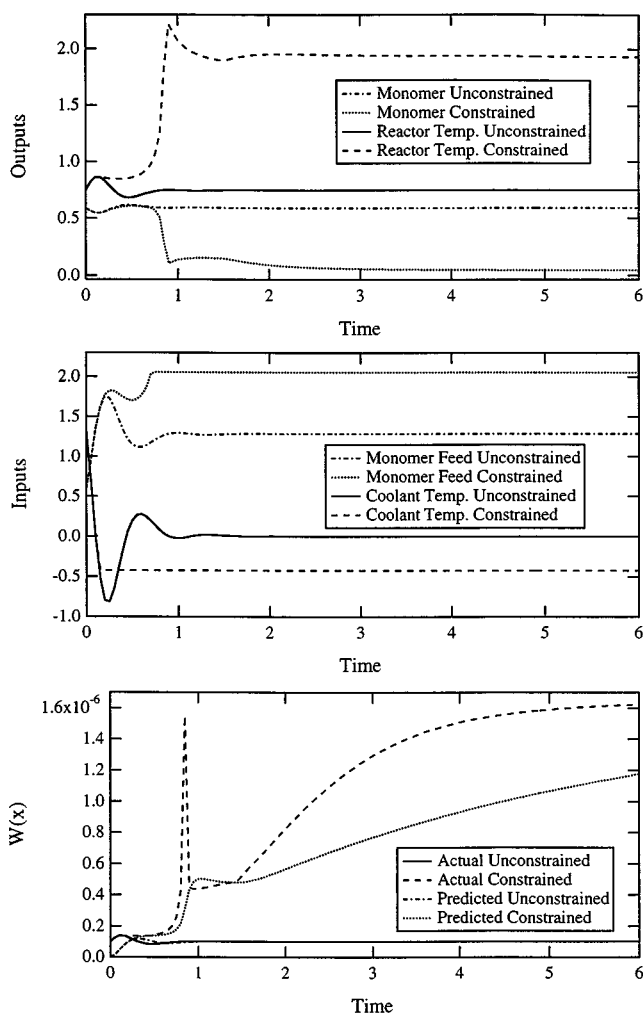


Fig. 2. Nominal point stabilization (FBL-PP).

absence of constraints. In this case, the perturbation is handled easily. It is important to note that the steady-state input values required to achieve the setpoints are within the constraint region defined by (33). The only way we found to make the controller stabilize the nominal point in the presence of constraints is to use tighter tuning such that the closed-loop system is at least twice as fast as the original case (i.e., the closed-loop time constant is 0.1 or less). Under such tuning, the constraints are barely encountered so the controller can recover from the initial perturbation.

Fig. 3 shows the response of the FBL-PP controller for a sequence of setpoint changes. At $\tau = 0$ the setpoints are changed from the nominal values in Table II to $y_{sp} = [1.2 \ 0.0865]^T$, and then changed again at $\tau = 4$ to $y_{sp} = [0.31 \ 1.06]^T$. The first setpoint corresponds to a step change to a lower conversion, while the second setpoint is a step change to a higher conversion as compared to the nominal point. The outputs are unable to attain the setpoints as a result of the constraints. Also shown in Fig. 3 is the FBL-PP response in the absence of constraints. In this case, the setpoint changes are tracked very effectively. As for the case of stabilization, the controller must be tuned much tighter to obtain stable responses under input constraints. Even under these conditions, the performance is highly degraded as compared to the FBL-MPC controller (see below) and even tighter

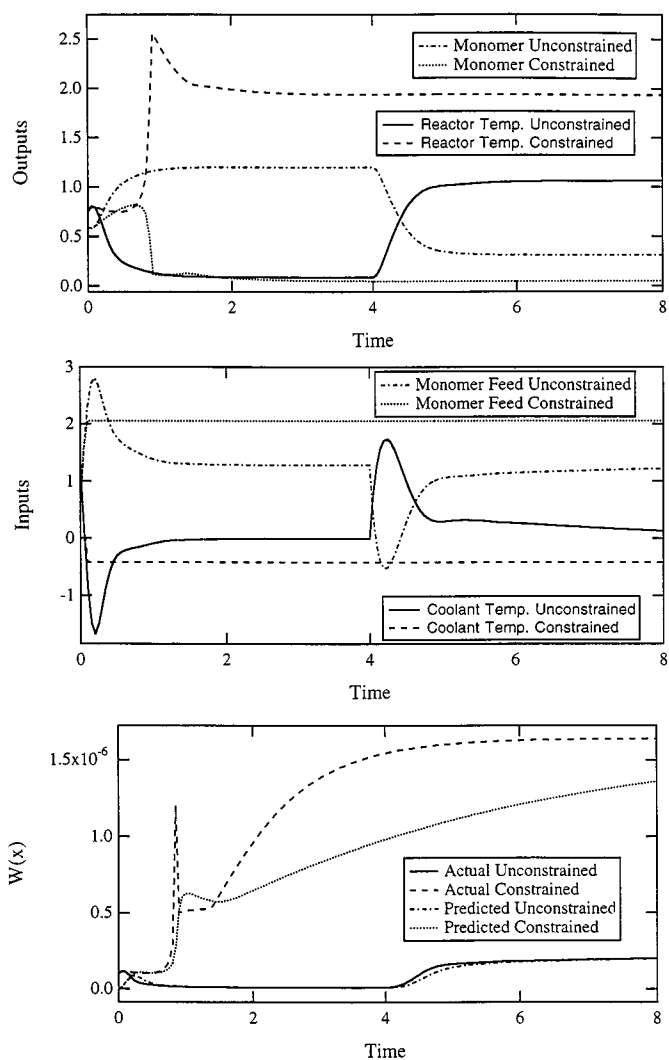


Fig. 3. Sequence of setpoint changes (FBL-PP).

tuning leads to complete failure. The “working region” of the FBL-PP controller corresponds to closed-loop time constants in the narrow range from 0.05 to 0.1. This is unacceptably small for an actual application.

The ability of the FBL-MPC controller to stabilize the nominal operating point in the presence of constraints is shown in Fig. 4. Despite the fact that constraints on both inputs are encountered, the FBL-MPC controller provides satisfactory performance. Note that the estimate of the live polymer concentration (W) converges rapidly to the true value. The closed-loop response for a sequence of setpoint changes with the FBL-MPC method is shown in Fig. 5. The setpoint changes are the same as those used in Fig. 3. The outputs smoothly track the setpoints despite the fact that the input constraints are encountered. The estimate of W effectively tracks the true value.

To compare the FBL-MPC control strategy to other nonlinear constraint handling techniques, a nonlinear antiwindup controller based on feedback linearization (FBL-AW) [10] and a nonlinear model predictive controller (NMPC) [13] are designed. The nonlinear antiwindup design is presented in [10]. In the present application, the multivariable antiwindup controller can be designed as two SISO antiwindup controllers

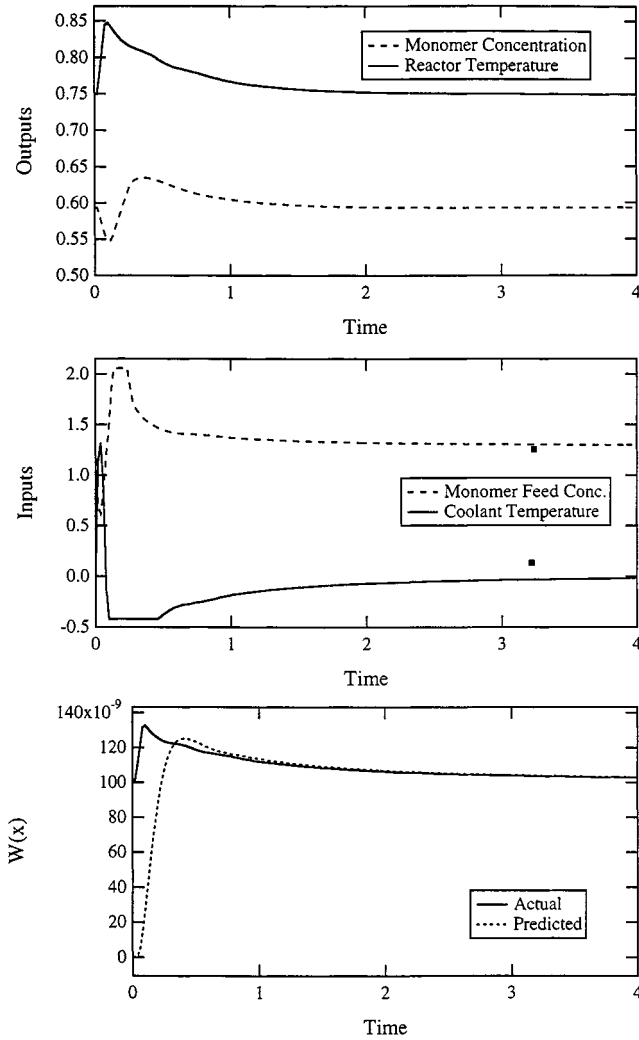


Fig. 4. Nominal point stabilization (FBL-MPC).

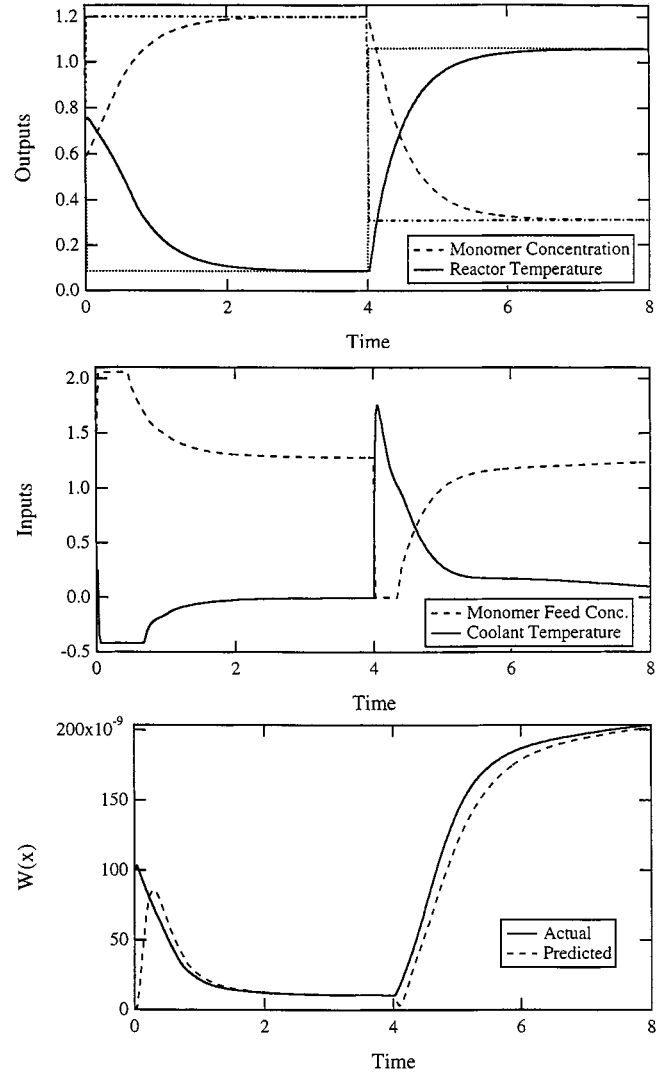


Fig. 5. Sequence of setpoint changes (FBL-MPC).

because the decoupling matrix is diagonal. The linear antiwindup compensator has the following components:

$$\begin{aligned} \tilde{P}(s) &= \begin{bmatrix} \frac{1}{\alpha_1 s + \alpha_0} & 0 \\ 0 & \frac{1}{\alpha_1 s + \alpha_0} \end{bmatrix} \\ Q_1(s) &= \begin{bmatrix} \frac{\alpha_1 s + \gamma}{\lambda s + 1} & 0 \\ 0 & \frac{\alpha_1 s + \gamma}{\lambda s + 1} \end{bmatrix} \\ Q_2(s) &= \begin{bmatrix} \frac{\gamma - \alpha_0}{\alpha_1 s + \alpha_0} & 0 \\ 0 & \frac{\gamma - \alpha_0}{\alpha_1 s + \alpha_0} \end{bmatrix} \end{aligned} \quad (35)$$

where $\tilde{P}(s)$ is the feedback linearized model after prestabilization, $Q_1(s)$ is the part of the compensator which penalizes the error between the output and its setpoint, and $Q_2(s)$ is the part of the compensator which penalizes calculated input moves outside the constraints. It is easy to verify that these components satisfy all of the requirements for internal stability as given by Zheng *et al.* [20]. The antiwindup controller is tuned to give a similar response to the FBL-MPC controller in the absence of constraints for the test shown in Fig. 6. The controller parameters are

$$\alpha_1 = 0.125, \quad \alpha_0 = 1, \quad \gamma = 2, \quad \lambda = 0.15. \quad (36)$$

The parameter estimator for W is tuned as for the FBL-PP and FBL-MPC controllers.

The nonlinear model predictive controller [13] has the objective function as shown in [(37)] at the bottom of the next page: with the tuning $N = 5$, $P = 10$, $Q = 20$, $S = 0.02$. A terminal state constraint [13] is not included because other tests (not shown) indicate that its inclusion does not improve the closed-loop response but does increase on-line computation. The sampling time of the NMPC controller is taken to be the same as the FBL-MPC controller ($T = 0.02$).

Figs. 6 and 7 show the response of the three nonlinear constraint handling techniques for a step change from the nominal values to $y_{sp} = [0.31 \ 1.06]^T$ at $\tau = 0$. This corresponds to a change to a higher conversion compared to the nominal point. Fig. 6 shows that the antiwindup controller fails completely despite the fact that it was tuned to give a similar response to the FBL-MPC controller in the absence of constraints. The antiwindup controller must be tuned to avoid the input constraints to achieve satisfactory setpoint tracking. However, it should be mentioned that the

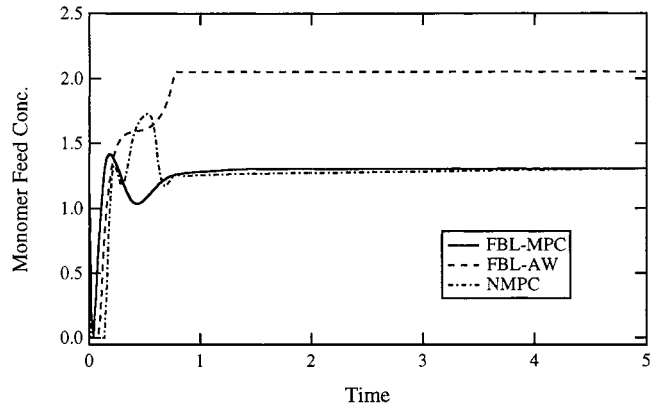
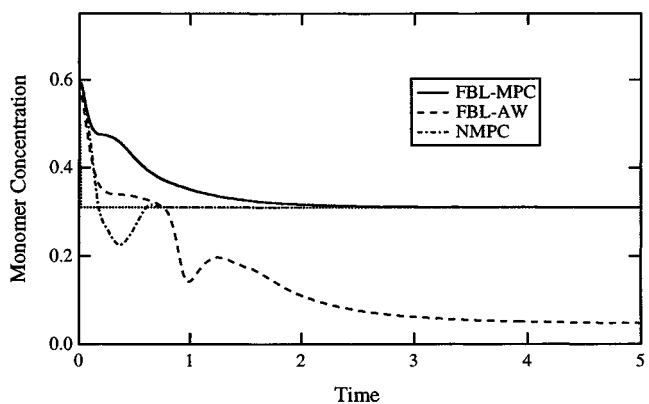
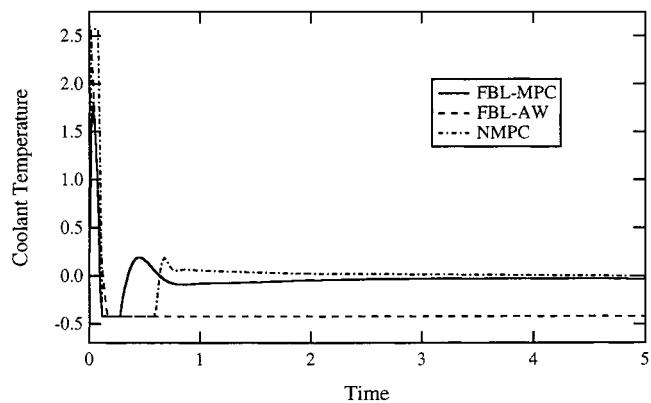
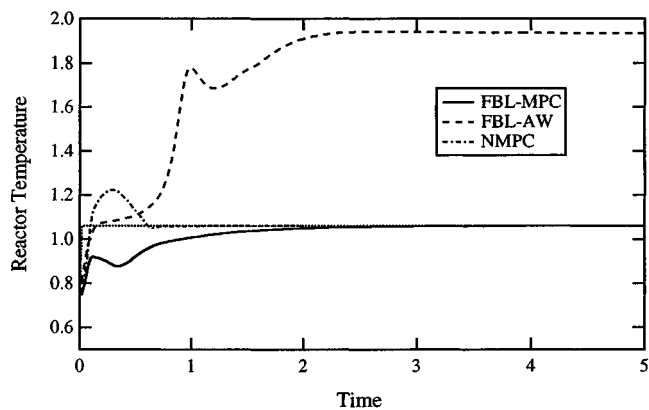


Fig. 6. Comparison of FBL-AW, FBL-MPC, and NMPC for a setpoint change to higher conversion.

Fig. 7. Inputs for Fig. 6.

FBL-AW controller did perform well in other tests such as the setpoint sequence shown in Fig. 5. The FBL-MPC controller provides good performance despite encountering the constraints. The NMPC controller provides excellent performance as the setpoints are reached significantly faster than with the FBL-MPC controller. On the other hand, the NMPC controller produces an appreciable overshoot.

The major shortcoming of the NMPC controller is computational overhead. For the test shown in Figs. 6 and 7, the approximate computation times on an IBM RS/6000 workstation running MATLAB are FBL-AW (3 min), FBL-MPC (30 min), and NMPC (24 h). The most computationally efficient algorithm is FBL-AW, which has a computation time about one-tenth that of FBL-MPC. The computation time for NMPC is approximately 40 times greater than that of FBL-MPC. It is important to note that a sampling time (T) of 0.02 dimensionless time units is used in these comparisons. Similar relationships would be ob-

tained for larger sampling times since computational time scales linearly with sampling time.

The closed-loop response obtained with the FBL-MPC controller for a disturbance in the reactor feed temperature (x_{2f}) is shown in Fig. 8. The value of x_{2f} is changed from its nominal value in Table II to 0.3 at $\tau = 3$. The disturbance is rejected effectively even though the coolant temperature temporarily saturates at its lower constraint. As before, the initial transient is due to the initialization error in \hat{W} . In this case the estimate of W is biased due to modeling error.

V. SUMMARY AND CONCLUSIONS

A nonlinear output feedback control strategy which explicitly accounts for input constraints has been developed for a multiple input–multiple output polymerization reactor. Input–output decoupling is used to obtain a linear model between the controlled outputs (monomer concentration and reactor temperature) and a

$$\begin{aligned}
 J = & \sum_{i=N}^{P-1} [y(k+i|k) - y_{sp}(k)]^T Q [y(k+i|k) - y_{sp}(k)] \\
 & + \sum_{i=0}^{N-1} \{ [y(k+i|k) - y_{sp}(k)]^T Q [y(k+i|k) - y_{sp}(k)] \\
 & + [u(k+i|k) - u(k+i-1|k)]^T S [u(k+i|k) - u(k+i-1|k)] \}
 \end{aligned} \tag{37}$$

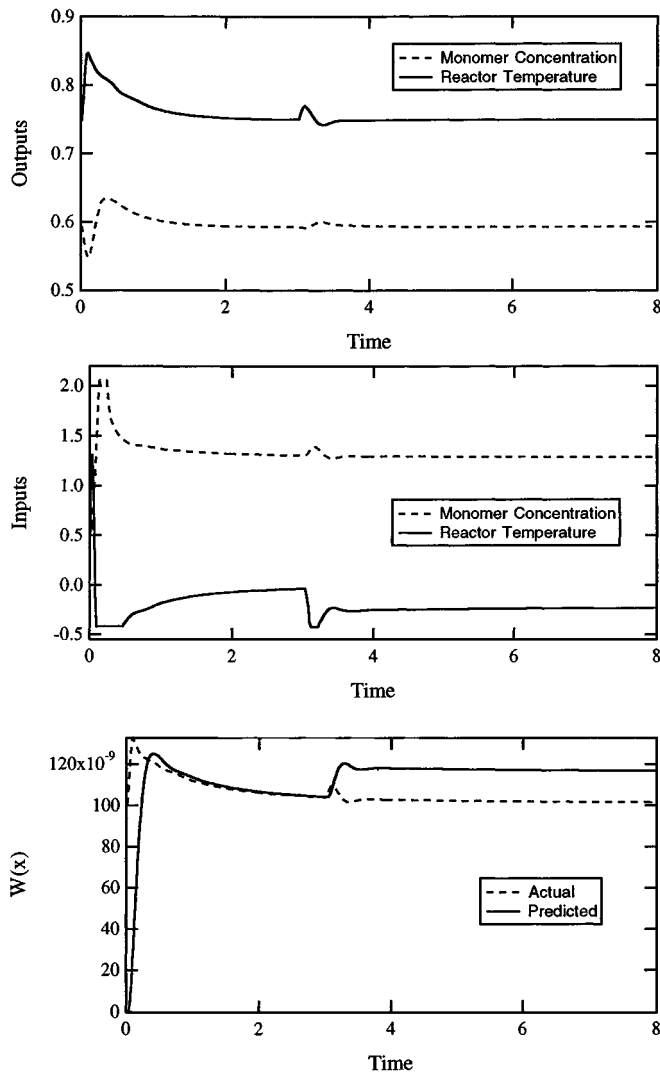


Fig. 8. Feed temperature disturbance (FBL-MPC).

vector of new manipulated inputs. Constraints on the actual manipulated inputs (monomer feed concentration and coolant temperature) are mapped into the feedback linearized space using the decoupling control law, and linear model predictive control is applied to the resulting constrained linear system. The unmeasured live polymer concentration is treated as an unknown parameter and estimated on-line using a gradient update law. Excellent servo and regulatory performance has been demonstrated via simulation. The proposed method offers superior performance as compared to a nonlinear anti windup controller and significantly reduced computational requirements as compared to a nonlinear model predictive controller.

REFERENCES

- [1] D. K. Adebekun and F. J. Schork, "Continuous solution polymerization reactor control. Part 1. Nonlinear reference control of methyl methacrylate polymerization," *Ind. Eng. Chem. Res.*, vol. 28, pp. 1308–1324, 1989.

- [2] —, "Continuous solution polymerization reactor control. Part 2. Estimation and nonlinear reference control during methyl methacrylate polymerization," *Ind. Eng. Chem. Res.*, vol. 28, pp. 1846–1861, 1989.
- [3] J. Alvarez, R. Suarez, and A. Sanchez, "Semiglobal nonlinear control based on complete input–output linearization and its application to the start-up of a continuous polymerization reactor," *Chem. Eng. Sci.*, vol. 49, pp. 3617–3630, 1994.
- [4] K. J. Astrom and B. Wittenmark, *Computer Controlled Systems: Theory and Design*, 2nd ed. Englewood Cliffs, NJ: Prentice-Hall, 1990.
- [5] P. Daoutidis, M. Soroush, and C. Kravaris, "Feedforward–feedback control of multivariable nonlinear processes," *AIChE J.*, vol. 36, pp. 1471–1484, 1990.
- [6] C. E. Garcia, "Quadratic dynamic matrix control of nonlinear processes: An application to a batch reactor process," *AIChE Annu. Meet.*, 1984.
- [7] M. A. Henson and D. E. Seborg, "Feedback linearizing control," in *Nonlinear Process Control*, M. A. Henson and D. E. Seborg, Eds. Englewood Cliffs, NJ: Prentice-Hall, 1997, ch. 4, pp. 149–232.
- [8] A. Isidori, *Nonlinear Control Systems*, 2nd ed. New York: Springer-Verlag, 1989.
- [9] G. Kalfas and W. H. Ray, "Modeling and experimental studies of aqueous suspension polymerization processes. Part 1. Modeling and simulations," *Ind. Eng. Chem. Res.*, vol. 32, pp. 1822–1830, 1993.
- [10] T. A. Kendi and F. J. Doyle, "An antiwindup scheme for input–output linearization," in *Proc. European Control Conf.*, Rome, Italy, 1995, pp. 2653–2658.
- [11] M. J. Kurtz and M. A. Henson, "Input–output linearizing control of constrained nonlinear processes," *J. Proc. Cont.*, vol. 7, pp. 3–17, 1997.
- [12] K. B. McAuley and J. F. MacGregor, "Nonlinear product property control in industrial gas-phase polyethylene reactors," *AIChE J.*, vol. 39, pp. 855–866, 1993.
- [13] E. S. Meadows and J. B. Rawlings, "Model predictive control," in *Nonlinear Process Control*, M. A. Henson and D. E. Seborg, Eds. Englewood Cliffs, NJ: Prentice-Hall, 1997, ch. 5, pp. 233–310.
- [14] K. R. Muske and T. F. Edgar, "Nonlinear state estimation," in *Nonlinear Process Control*, M. A. Henson and D. E. Seborg, Eds. Englewood Cliffs, NJ: Prentice-Hall, 1997, ch. 6, pp. 311–370.
- [15] K. R. Muske and J. B. Rawlings, "Model predictive control with linear models," *AIChE J.*, vol. 39, pp. 262–287, 1993.
- [16] W. H. Ray, "Polymerization reactor control," *IEEE Contr. Syst.*, vol. 6, pp. 3–8, 1986.
- [17] S. Sastry and M. Bodson, *Adaptive Control: Stability, Convergence, and Robustness*. Englewood Cliffs, NJ: Prentice-Hall, 1989.
- [18] A. D. Schmidt and W. H. Ray, "The dynamic behavior of continuous polymerization reactors—I," *Chem. Eng. Sci.*, vol. 36, pp. 1401–1410, 1981.
- [19] M. Soroush and C. Kravaris, "Multivariable nonlinear control of a continuous polymerization reactor: An experimental study," *AIChE J.*, vol. 39, pp. 1920–1937, 1993.
- [20] A. Zheng, M. Kothare, and M. Morari, "Antiwindup design for internal model control," *Int. J. Contr.*, vol. 60, pp. 1015–1024, 1994.



Michael J. Kurtz received the B.S. degree in chemical engineering from Florida State University, Tallahassee, in 1993 and the Ph.D. degree in chemical engineering from Louisiana State University, Baton Rouge, in 1997.

He currently is an Applications Engineer for Exxon Chemical Company, Baton Rouge, working in the elastomers group. His current research interests include the development of nonlinear control strategies for chemical process applications as well as statistical data validation for polymerization

systems.



Guang-Yan Zhu received the B.S. degree in chemical engineering from the University of South Florida, Tampa, in 1996, where he graduated magna cum laude and was named the Outstanding Graduate of the College of Engineering. He is currently a Ph.D. candidate at Louisiana State University, Baton Rouge

He worked for U.S. Agri-Chemical Company during and after his undergraduate education. His research interests include model predictive control of nonlinear systems, biochemical reactor modeling and control using population balance equations, and modeling and control of industrial gas pipeline networks.



Michael A. Henson (S'90–M'92) received the B.S. degree in chemical engineering from University of Colorado, Boulder, in 1985, the M.S. degree in chemical engineering from University of Texas, Austin, in 1988, and the Ph.D. degree in chemical engineering from University of California, Santa Barbara, in 1992.

He held the position of Visiting Research Scientist with the DuPont Company from 1992 to 1993. He currently is an Associate Professor of Chemical Engineering at Louisiana State University. He is a coeditor of the book *Nonlinear Process Control* (Englewood Cliffs, NJ: Prentice-Hall, 1997) and has authored over 50 book chapters, journal articles, and conference proceedings papers. His current research interests include the development of nonlinear and adaptive control strategies for chemical and biochemical process applications.

Dr. Henson received an Early Faculty Career Development Award from the National Science Foundation in 1995. He served as an Associate Editor of the IEEE Control Systems Society Conference Editorial Board from 1994 to 1996.